NASA Technical Memorandum 101499

DYNAMIC EVALUATION OF A TRACTION-DRIVE JOINT FOR SPACE TELEROBOTS

Clarence W. deSilva and
Walter W. Hankins III

October 1988

National Aeronautics and
Space Administration

Langley Research Center
Hampton, Virginia 23665-5225

TABLE OF CONTENTS

DYNAMIC EVALUATION OF A TRACTION-DRIVE JOINT FOR SPACE TELEROBOTS

Clarence W. deSilva* and Walter W. Hankins III

ABSTRACT

This paper presents an analysis and evaluation of a prototype traction-drive joint for robotic manipulators, developed under the sponsorship of NASA. A dynamic model is developed using the Lagrange formulation. Controllability, observability, dynamic stability, and response characteristics of the joint to test inputs are studied. A linear quadratic regulator (LQR) is implemented on the joint model to determine a basis for evaluating the performance of the traction-drive joint under servo control. An evaluation of the results and directions for future investigations are presented.

*NSERC Professor of Industrial Automation, Department of Mechanical Engineering, University of British Columbia

SYMBOLS

Scalar Parameters

b_1 - combined damping constant at the motor and drive side of the speed reducer (oz.in/rad/s)

b_2 - combined damping constant at the driven side of the speed reducer and input side of the drive roller (oz.in/rad/s)

b_3 - damping constant at the output side of the drive roller (oz.in/rad/s)

b_4 - damping constant at a differential wheel (oz.in/rad/s)

b_{51} - roll (yaw) damping constant at the output member (oz.in/rad/s)

b_{52} - pitch damping constant at the roll output member (oz.in/rad/s)

b_6 - pitch damping constant of the output coupling member (oz.in/rad/s)

J_1 - combined inertia of the motor rotor and drive side of the speed reducer (oz.in.s^2)

J_2 - combined inertia of the driven side of the speed reducer and input side of the drive roller (oz.in.s^2)

J_3 - inertia of the output side of the drive roller (oz.in.s^2)

J_4 - inertia of one differential wheel (oz.in.s^2)

J_{51} - roll (yaw) inertia of the output member (oz.in.s^2)

J_{52} - pitch inertia of the roll member (oz.in.s^2)

J_6 - pitch inertia of the output coupling member (oz.in.s^2)

J_c - roll-pitch cross inertia of the output member (oz.in.s^2)

K - torsional stiffness of the drive roller (oz.in/rad)

L - lagrangian of the joint (oz.in)

n_r - speed ratio of the motor speed reducer

n_1 - speed ratio of the differential

Q_i - generalized force associated with the coordinate θ_i (oz.in)

T - kinetic energy of the joint (oz.in.rad)

T_2 - torque through the second drive roller (oz.in)

T_{m1} - output torque of the first servomotor (oz.in)

T_{m2} - output torque of the second servomotor (oz.in)

u_i - an input variable

V - potential energy of the joint (oz.in.rad)

W - virtual work (oz.in.rad)

x_i - a state variable

y_i - an output variable

Vectors and Matrices

$\underline{A}$ - system matrix

$\underline{B}$ - input distribution matrix

$\underline{C}$ - output (measurement) gain matrix

$\underline{D}$ - feedforward gain matrix

$\underline{u}$ - input vector

$\underline{x}$ - state vector

$\underline{y}$ - output vector

Greek Symbols

θ_1 - angle of rotation of the first motor

θ_2 - angle of rotation of the second motor

θ_3 - output angle of the first drive roller

θ_4 - output angle of the second drive roller

ψ - roll (yaw) output angle of the joint

ϕ - pitch output angle of the joint

INTRODUCTION

Most industrial robots are open-link chains driven by actuating the link joints of a manipulator. DC motors, AC synchronous motors, induction motors, stepping motors, or hydraulic actuators may be used as the joint actuators. Since conventional motors provide speeds that are too high for most robotic tasks and since high driving torques are desirable, speed reducers such as gear transmissions, timing belts, and sprocket and chain devices are usually incorporated at the manipulator joints. gear transmissions can introduce backlash, which can result in low stiffness, degraded accuracy and repeatability, accelerated wear, noise and vibration, and dynamic and control problems, including limit cycle response. Backlash can be reduced using special gear designs. Harmonic drives, for example [1], incorporate preloading at the tooth mesh region, but this can increase friction and local stresses.

Direct-drive manipulators use high-torque, low-speed DC motors without gear reducers [2, 3]. They are known to have low levels of joint friction and practically no backlash. Unfortunately, however, a direct-drive joint tends to be considerably heavier than a conventional joint having comparable capabilities. This would demand stronger and heavier links with associated reductions in bandwidth and increased flexibility problems.

Recently, the use of traction (friction) drive has been proposed as an alternative to gear transmission, and a manipulator using traction drives for the joints is being developed [4]. This promises improvements in the manipulator performance in terms of accuracy and efficiency. In particular, backlash problems would be virtually nonexistent and the frictional disspation would be small. Futhermore, it has the potential for high stiffness and smooth operation, with overload protection naturally built in to the joint through the friction-drive mechanism. However, traction drives are known to have two disadvantages. They are bigger and heavier than gear transmissions and practical experience with them is limited.

This paper presents a dynamic analysis and evaluation of a traction-drive joint, particularly from the control point of view. A dynamic model is developed for the joint. Its behavior is evaluated using controllability, observability, stability, and response analyses. Next the servo control problem of a single joint is studied in terms of the required outputs for the feedback servo and with regard to the optimal performance.

LABORATORY TELEROBOTIC MANIPULATOR

System Design

NASA Langley Research Center is currently sponsoring construction of a Laboratory Telerobotic Manipulator (LTM) by the Department of Energy's Oak Ridge National Laboratory [4]. LTM will be able to be operated as a dual arm force-reflecting master/slave teleoperator, or as a robot, using distributed high-speed microprocessors. LTM has redundant kinematics, supplied by differential traction drives at the shoulder, elbow and wrist joints, plus a seventh (roll) degree of freedom at the wrist (fig. 1).

Differential Traction Drive Joint

Figure 2 is a schematic drawing of the LTM traction-drive joint. Figure 3(a) shows a traction drive differential test fixture. A close-up of the drive rollers is shown in figure 3(b). The two input rollers are frictionally engaged with two intermediate wheels of much larger diameter, which form a differential mechanism. These two differential wheels are in turn frictionally engaged with a single output roller. When the two differential wheels rotate in opposite directions at the same speed, the output roller will undergo a roll motion about its axis. When the two differential wheels rotate in the same direction at equal speeds, the output roller will pitch without any rolling motion. In this manner two degrees of freedom are provided by a single joint. Note that the roll motion of the output roller can be interpreted as a yaw motion if the output shaft is bent through 90 degrees. Also, any combination of yaw and pitch motions can be produced at the output of the joint simply by adjusting the motions of the two input rollers which are driven using DC servo motors. Digital shaft encoders for position (and speed) sensing, tachometers for analog speed sensing, and torque sensors are incorporated in each axis. These sensors will provide the feedback signals for the operation of the joint servo.

DYNAMIC MODEL

Lagrange Equations

The traction-drive joint described in the previous section may be modeled as in Figure 4. Motor torques, not drive voltages, are used as the inputs to the joint. The rationale here is that the coupling of the motor back e.m.f. can be compensated by using a local current feedback loop in the drive amplifier. The Lagrange energy method is used to establish the dynamic equations for the joint. Joint backlash is neglected, and energy dissipation is modeled as viscous damping. Flexibility of the input drive roller is represented by a torsional stiffness K. Other moving components are individually assumed to be rigid. The moment of inertia of each such component is denoted by J, with a suitable subscript. Each inertia component will also have an associated damping constant that is denoted by b with the same subscript. Suppose:

J_1 = combined inertia of motor rotor and drive side of the speed reducer

J_2 = combined inertia of the driven side of the speed reducer and input side of the drive roller

J_3 = inertia of the output side of the drive roller

J_4 = inertia of one differential wheel

The output member has two axes of rotation, denoted as roll axis and pitch axis in figure 4. This member actually consists of two rigid components. The output shaft that is directly engaged with the differential wheels has an inertia J_{51} about the roll (yaw) axis and an inertia J_{52} about the pitch axis. The cross member transmits the pitch motion of the output shaft and it has a pitch inertia of J_6. This member does not undergo a roll (yaw) motion. It follows that by considering the two orthogonal axes of motion (roll and pitch), the inertia matrix of the combined output member may be expressed as

$$\begin{bmatrix} J_{51} & J_c \\ J_c & J_{52} \end{bmatrix}$$

in which J_c is the cross inertia that represents the inertial coupling between the two axes, resulting from the fact that the roll axis and the pitch axis are not the principal axes of inertia of the output member, in general.

Suppose θ_1 and θ_2 denote the angles of rotation of the two motors, and θ_3 and θ_4 be the angles of rotation at the output ends of the drive rollers, as indicated in Figure 4. If n_R is the gear ratio of the speed reducer, the rotations at the input ends of the drive rollers will be θ_1/n_R and θ_2/n_R as shown. Also, θ_3/n_1 and θ_4/n_1 will be the rotations of the differential wheels, n_1 being the transmission ratio from the drive roller to the differential wheel. We can decompose each of these angles into two components as

$$\frac{\theta_3}{n_1} = \frac{(\theta_3 + \theta_4)}{2n_1} + \frac{(\theta_3 - \theta_4)}{2n_1} \tag{1}$$

$$\frac{\theta_4}{n_1} = \frac{(\theta_3 + \theta_4)}{2n_1} - \frac{(\theta_3 - \theta_4)}{2n_1} \tag{2}$$

Note that the first component on the right hand side of each equation represents differential wheel rotations through the same angle in the same direction and the second component represents differential wheel rotations through the same angle in opposite directions. Now assuming the transmission ratio from the differential wheels to the output member to be unity along both roll and pitch axes we observe that the roll (yaw) angle is

$$\psi = \frac{\theta_3 + \theta_4}{2n_1} \tag{3}$$

and the pitch angle is

$$\phi = \frac{\theta_3 - \theta_4}{2n_1} \tag{4}$$

Kinetic energy of the output member is given by

$$\frac{1}{2}\begin{bmatrix} \frac{(\dot\theta_3 + \dot\theta_4)}{2n} & \frac{(\dot\theta_3 - \dot\theta_4)}{2n} \end{bmatrix}\begin{bmatrix} J_{51} & J_c \\ J_c & J_{52} \end{bmatrix}\begin{bmatrix} (\dot\theta_3 + \dot\theta_4)/(2n_1) \\ (\dot\theta_3 - \dot\theta_4)/(2n_1) \end{bmatrix}$$

$$= \frac{1}{2}J_{51}\left[\frac{\dot\theta_3 + \dot\theta_4}{2n_1}\right]^2 + \frac{1}{2}J_{52}\left[\frac{\dot\theta_3 - \dot\theta_4}{2n_1}\right]^2 + J_c\frac{(\dot\theta_3^2 - \dot\theta_4^2)}{4n_1^2}$$

The overall kinematic energy of the entire joint is given by

$$T = \frac{1}{2} J_1 \dot{\theta}_1^2 + \frac{1}{2} J_2 \left[\frac{\dot{\theta}_1}{n_r}\right]^2 + \frac{1}{2} J_3 \dot{\theta}_3^2 + \frac{1}{2} J_4 \left[\frac{\dot{\theta}_3}{n_1}\right]^2$$

$$+ \frac{1}{2} J_1 \dot{\theta}_2^2 + \frac{1}{2} J_2 \left[\frac{\dot{\theta}_2}{n_r}\right]^2 + \frac{1}{2} J_3 \dot{\theta}_4^2 + \frac{1}{2} J_4 \left[\frac{\dot{\theta}_3}{n_1}\right]^2$$

$$+ \frac{1}{2} J_{51} \left[\frac{\dot{\theta}_3 + \dot{\theta}_4}{2n_1}\right]^2 + \frac{1}{2} (J_{52} + J_6) \left[\frac{\dot{\theta}_3 - \dot{\theta}_4}{2n_1}\right]^2 + J_c \frac{(\dot{\theta}_3^2 - \dot{\theta}_4^2)}{4n_1^2} \tag{5}$$

Next denoting the torsional stiffness of the drive roller by K, the potential energy of the entire unit may be expressed as

$$V = \frac{1}{2} K \left[\frac{\theta_1}{n_r} - \theta_3\right]^2 + \frac{1}{2} K \left[\frac{\theta_2}{n_r} - \theta_4\right]^2 \tag{6}$$

Note that gravity terms have been neglected in this expression; we are concerned with microgravity operation of the joint in space applications.

The Lagrangian L is formed according to

$$L = T - V \tag{7}$$

in which θ_1, θ_2, θ_3, and θ_4 form a complete set of generalized coordinates for the joint. Then the equations of motion for the joint are obtained by forming the Lagrange equations:

$$\frac{d}{dt} \frac{\partial L}{\partial \dot{\theta}_i} - \frac{\partial L}{\partial \theta_i} = Q_i \tag{8}$$

for $i = 1, 2, 3,$ and 4.

It remains to obtain expressions for the generalized forces Q_i. To do this the generalized coordinates are incremented and the resulting virtual work δW due to the nonconservative forces (torques) is determined. The associated virtual work is given by

$$\delta W = T_{m1} \delta\theta_1 + T_{m2} \delta\theta_2 - b_1 \dot{\theta}_1 \delta\theta_1 - b_1 \dot{\theta}_2 \delta\theta_2 - b_2 \frac{\dot{\theta}_1}{n_R} \frac{\delta\theta_1}{n_R} - b_2 \frac{\dot{\theta}_2}{n_R} \frac{\delta\theta_2}{n_R}$$

$$- b_3 \dot{\theta}_3 \delta\theta_3 - b_3 \dot{\theta}_4 \delta\theta_4 - b_4 \frac{\dot{\theta}_3}{n_1} \frac{\delta\theta_3}{n_1} - b_4 \frac{\dot{\theta}_4}{n_1} \frac{\delta\theta_4}{n_1}$$

$$- b_{51} \frac{(\dot{\theta}_3 + \dot{\theta}_4)(\delta\theta_3 + \delta\theta_4)}{2n_1} \frac{}{2n_1} - b_{52} \frac{(\dot{\theta}_3 - \dot{\theta}_4)(\delta\theta_3 - \delta\theta_4)}{2n_1} \frac{}{2n_1} - b_6 \frac{(\dot{\theta}_3 - \dot{\theta}_4)(\delta\theta_3 - \delta\theta_4)}{2n_1} \frac{}{2n_1}$$

$$= Q_1 \delta\theta_1 + Q_2\delta\theta_2 + Q_3\delta\theta_3 + Q_4 \delta\theta_4 \tag{9}$$

Note that Q_i are determined simply by comparing the two sides of equation (9). Finally, by combining all these results the following Lagrange equations of motion are obtained:

$$\left[J_1 + \frac{J_2}{n_R^2}\right]\ddot{\theta}_1 + \left[b_1 + \frac{b_2}{n_R^2}\right]\dot{\theta}_1 + \frac{K}{n_R^2}\theta_1 - \frac{K}{n_R}\theta_3 = T_{m1} \tag{10}$$

$$J_1 + \frac{J_2}{n_R^2}\ddot{\theta}_2 + b_1 + \frac{b_2}{n_R^2}\dot{\theta}_2 + \frac{K}{n_R^2}\theta_2 - \frac{K}{n_R}\theta_4 = T_{m2} \tag{11}$$

$$\left[J_3 + \frac{J_4}{n_1^2} + \frac{(J_{51} + J_{52} + J_6)}{4n_1^2} + \frac{J_c}{2n_1^2}\right]\ddot{\theta}_3 + \left[\frac{J_{51} - J_{52} - J_6}{4n_1^2}\right]\ddot{\theta}_4$$

$$+ \left[b_3 + \frac{b_4}{n_1^2} + \frac{(b_{51} + b_{52} + b_6)}{4n_1^2}\right]\dot{\theta}_3 + \left[\frac{b_{51} - b_{52} - b_6}{4n_1^2}\right]\dot{\theta}_4 - K\theta_3 - \frac{K}{n_R}\theta_1 = 0 \tag{12}$$

$$\left[J_3 + \frac{J_4}{n_1^2} + \frac{J_{51} + J_{52} + J_6}{4n_1^2} - \frac{J_c}{2n_1^2}\right]\ddot{\theta}_4 + \left[\frac{J_{51} - J_{52} - J_6}{4n_1^2}\right]\ddot{\theta}_3$$

$$+ \left[b_3 + \frac{b_4}{n_1^2} + \frac{(b_{51} + b_{52} + b_6)}{4n_1^2}\right]\dot{\theta}_4 + \left[\frac{b_{51} - b_{52} - b_6}{4n_1^2}\right]\dot{\theta}_3 + K\theta_4 - \frac{K}{n_R}\theta_2 = 0 \tag{13}$$

It is desirable to eliminate the variables θ_3 and θ_4 using the roll angle ψ and the pitch angle ϕ. This can be accomplished by manipulating the last two equations of motion given above. First, for brevity, define the following parameters:

$$J_{1eq} = J_1 + \frac{J_2}{n_R^2} \tag{14}$$

$$J_{2eq} = J_3 + \frac{J_4}{n_1^2} + \frac{(J_{51} + J_{52} + J_6)}{4n_1^2} \tag{15}$$

$$J_{3eq} = \frac{J_{52} + J_6 - J_{51}}{4n_1^2} \tag{16}$$

$$J_{ceq} = \frac{J_c}{2n_1^2} \tag{17}$$

Also, b_{1eq}, b_{2eq}, and b_{3eq} are defined in an analogous manner. Then the dynamic equations for the joint can be written as

$$J_{1eq}\ddot{\theta}_1 + b_{1eq}\dot{\theta}_1 + \frac{K}{n_R^2}\theta_1 - \frac{Kn_1}{n_R}(\psi + \phi) = T_{m1} \tag{18}$$

$$J_{1eq}\ddot{\theta}_2 + b_{1eq}\dot{\theta}_2 + \frac{K}{n_R^2}\theta_2 - \frac{Kn_1}{n_R}(\psi - \phi) = T_{m2} \tag{19}$$

$$(J_{2eq} - J_{3eq})\ddot{\psi} + J\ddot{\phi} + (b_{2eq} - b_{3eq})\dot{\psi} + K\psi - \frac{K}{2n_1n_R}(\theta_1 + \theta_2) = 0 \tag{20}$$

$$(J_{2eq} + J_{3eq})\ddot{\phi} + J\ddot{\psi} + (b_{2eq} + b_{3eq})\dot{\phi} + K\phi - \frac{K}{2n_1n_R}(\theta_1 - \theta_2) = 0 \tag{21}$$

State Space Model

The equations of motion developed in the previous section represent a coupled, four-degree-of-freedom, eighth order model with two inputs T_{m1} and T_{m2}. Since it is convenient to use multivariable techniques for analysis and control of systems of this type, we wish to express the model in the state space form. An assumption that would considerably simplify the formulation is that J_{ceq} is negligible in comparison to the remaining inertia parameters. This assumption is justified here because the cross inertia term J_c is usually small compared to the direct inertia terms and because the transmission ratio n_1 is larger than unity. Accordingly, J_{ceq} is neglected in the analysis that follows.

The state space model is given by

$$\dot{\underline{x}} = \underline{A}\underline{x} + \underline{B}\underline{u} \tag{22}$$

$$\underline{y} = \underline{C}\underline{x} + \underline{D}\underline{u} \tag{23}$$

The state vector $\underline{x}$ is defined as

$$\underline{x} = [\theta_1, \dot{\theta}_1, \theta_2, \dot{\theta}_2, \psi, \dot{\psi}, \phi, \dot{\phi}]^T \tag{24}$$

and the input vector $\underline{u}$ is given by

$$\underline{u} = [T_{m1}, T_{m2}]^T \tag{25}$$

Torques transmitted through the two drive rollers, as measured by the torque sensors, and the roll (yaw) angle and the pitch angle, as measured by the roll and pitch encoders, are taken as the system outputs:

$$y_1 = T_1 = K(\theta_1/n_R - \theta_3) = K(x_1/n_R - n_1 x_5 - n_1 x_7) \tag{26}$$

$$y_2 = T_2 = K(\theta_2/n_R - \theta_4) = K(x_3/n_R - n_1 x_5 + n_1 x_7) \tag{27}$$

$$y_3 = \psi = x_5 \tag{28}$$

$$y_4 = \phi = x_7 \tag{29}$$

With this choice of variables, the system matrix is given by

$$\underline{A} = \begin{bmatrix} 0 & 1 & 0 & 0 & 0 & 0 & 0 & 0 \\ -a_1 & -a_2 & 0 & 0 & a_3 & 0 & a_3 & 0 \\ 0 & 0 & 0 & 1 & 0 & 0 & 0 & 0 \\ 0 & 0 & -a_1 & -a_2 & a_3 & 0 & -a_3 & 0 \\ 0 & 0 & 0 & 0 & 0 & 1 & 0 & 0 \\ a_4 & 0 & a_4 & 0 & -a_5 & -a_6 & 0 & 0 \\ 0 & 0 & 0 & 0 & 0 & 0 & 0 & 1 \\ a_7 & 0 & -a_7 & 0 & 0 & 0 & -a_8 & -a_9 \end{bmatrix} \tag{30}$$

the input distribution matrix is given by

$$\underline{B} = \begin{bmatrix} 0 & 0 \\ 1/J_{1eq} & 0 \\ 0 & 0 \\ 0 & 1/J_{1eq} \\ 0 & 0 \\ 0 & 0 \\ 0 & 0 \\ 0 & 0 \end{bmatrix} \tag{31}$$

and the output gain matrix is given by

$$\underline{C} = \begin{bmatrix} K/n_R & 0 & 0 & 0 & -Kn_1 & 0 & -Kn_1 & 0 \\ 0 & 0 & K/n_R & 0 & -Kn_1 & 0 & Kn_1 & 0 \\ 0 & 0 & 0 & 0 & 1 & 0 & 0 & 0 \\ 0 & 0 & 0 & 0 & 0 & 0 & 1 & 0 \end{bmatrix} \tag{32}$$

Note that there are no feedforward paths in the model. Accordingly,

$$\underline{D} = \underline{0} \tag{33}$$

Also the following parameters have been defined:

$$a_1 = \frac{K}{J_{1eq} n_R^2} \tag{34}$$

$$a_2 = \frac{b_{1eq}}{J_{1eq}} \tag{35}$$

$$a_3 = \frac{Kn_1}{J_{1eq} n_R} \tag{36}$$

$$a_4 = \frac{K}{2n_1 n_R (J_{2eq} - J_{3eq})} \tag{37}$$

$$a_5 = \frac{K}{(J_{2eq} - J_{3eq})} \tag{38}$$

$$a_6 = \frac{(b_{2eq} - b_{3eq})}{(J_{2eq} - J_{3eq})} \tag{39}$$

$$a_7 = \frac{K}{2n_1 n_R (J_{2eq} + J_{3eq})} \tag{40}$$

$$a_8 = \frac{K}{(J_{2eq} + J_{3eq})} \tag{41}$$

$$a_9 = \frac{(b_{2eq} + b_{3eq})}{(J_{2eq} + J_{3eq})} \tag{42}$$

This state space model will be used in the subsequent study of the traction-drive joint.

PERFORMANCE EVALUATION

Parameter Values

Parameter values are chosen in consultation with Oak Ridge National Laboratory and product data sheets, to represent the true inertia, stiffness, and damping properties of the joint. The following values are used

$J_1 = 0.04$ oz.in.s^2
$J_2 = 0.07$ oz.in.s^2
$J_3 = 0.03$ oz.in.s^2
$J_4 = 0.10$ oz.in.s^2
$J_{51} = 0.80$ oz.in.s^2
$J_{52} = 0.40$ oz.in.s^2
$J_6 = 0.50$ oz.in.s^2
$n_R = 30$ $\quad n_1 = 3.75$
$K = 30000.0$ oz.in/rad

$b_1 = 0.003$ oz.in/rad/s
$b_2 = 0.004$ oz.in/rad/s
$b_3 = 0.003$ oz.in/rad/s
$b_4 = 0.003$ oz.in/rad/s
$b_{51} = 0.003$ oz.in/rad/s
$b_{52} = 0.003$ oz.in/rad/s
$b_6 = 0.003$ oz.in/rad/s

With these numerical values the matrices of the state space model become

$$\underline{A} = \begin{bmatrix} 0 & 0 & 0 & 0 & 0 & 0 & 0 & 0 \\ -830. & 0 & 0 & 0 & 93570. & 0 & 93570. & 0 \\ 0 & 0 & 0 & 0 & 0 & 0 & 0 & 0 \\ 0 & 0 & -830. & 0 & 93570. & 0 & -93570. & 0 \\ 0 & 0 & 0 & 0 & 0 & 0 & 0 & 0 \\ 2030. & 0 & 2030. & 0 & -457630. & 0 & 0 & 0 \\ 0 & 0 & 0 & 0 & 0 & 0 & 0 & 0 \\ 1930. & 0 & -1930. & 0 & 0 & 0 & -434080. & 0 \end{bmatrix}$$

$$\underline{B} = \begin{bmatrix} 0 & 0 \\ 24.9515 & 0 \\ 0 & 0 \\ 0 & 24.9515 \\ 0 & 0 \\ 0 & 0 \\ 0 & 0 \\ 0 & 0 \end{bmatrix}$$

and

$$\underline{C} = \begin{bmatrix} 1000. & 0 & 0 & 0 & -112500. & 0 & -112500. & 0 \\ 0 & 0 & 1000. & 0 & -112500. & 0 & 112500. & 0 \\ 0 & 0 & 0 & 0 & 1.0 & 0 & 0 & 0 \\ 0 & 0 & 0 & 0 & 0 & 0 & 1.0 & 0 \end{bmatrix}$$

A commercially available software package for analysis and design of control systems is used in the studies described below. First the joint model is programmed in to the system using the DIARY capability of the software package. Next controllability, observability, stability, and response studies will be conducted. Finally control studies will be performed.

Controllability

A system is said to be controllable if its state vector can be changed from some arbitrary initial vector value to any arbitrary final (vector) value in a finite time

and using a finite control effort [2]. This is indeed a requirement for any well-behaved control system. For the present case of time invariant systems the necessary and sufficient condition for controllability is

$$\text{Rank } [\underline{B},\ \underline{A}\ \underline{B},\ \underline{A}^2\underline{B},\ \ldots.,\ \underline{A}^{n-1}\underline{B}] = n \tag{43}$$

in which n is the order of the system. For the joint model developed here, $n = 8$, and it was verified that the controllability condition is satisfied. This means that we should be able to realize any joint response that we desire or able to control the joint in any manner by using appropriate inputs.

Observability

The joint model developed in this paper has eight states and four outputs. If all eight states can be measured and used in controlling the joint, it is known that the joint can be controlled in an optimal manner, and that stability of the system can be improved in an arbitrary manner. But it is not always possible or convenient to measure all state variables in a system. Then the question arises whether it is possible to determine the value of the state vector at any arbitrary instant by measuring the output vector from that instant for a finite period of time. The system is said to be observable if and only if this is possible [2].

For the time-invariant model developed here, the necessary and sufficient condition for observability is

$$\text{Rank } [\underline{C}^T,\ \underline{A}^T\underline{C}^T,\ (\underline{A}^T)^2\ \underline{C}^T,\ \ldots.,\ (\underline{A}^T)^{n-1}\underline{C}^T] = n \tag{44}$$

It was verified that the traction-drive joint as defined above, is observable. It follows that output feedback can be substituted for complete-state feedback without compromising the joint performance. It can be concluded that the four outputs defined in the state model are quite adequate for servoing the joint.

Further study revealed that the system is observable with the two motion variables (roll and pitch angles) alone. This indicates that the torque sensing is not needed, in theory, to completely control the joint. In practice, however, torque sensing might be quite useful. For example, a hybrid control scheme consisting of both motion feedback and torque feedback could considerably improve the performance of the joint under load disturbances, unknown parameters, and when fine manipulation under very tight motion tolerances is needed as in the case of parts assembly or in manipulations under motion constraints where damaging forces could arise even with small motion errors.

It was found that the system is not completely observable when only one of the two motion variables is measured. In this case only four of the eight state variables can be estimated. It follows that roll angle and pitch angle both are needed for servoing the joint.

Stability

Stability is determined by the eigenvalues of the system matrix. Without any feedback control, the eigenvalues of $\underline{A}$ are found to be

$-0.03 \pm j\ 677.10$
$-0.02 \pm j\ 659.48$
-0.07
-0.07
0.0
0.0

It is noted that the open-loop system is marginally stable, as indicated by the zero eigenvalues. This is to be expected in view of the fact that the joint is driven by two actuators each of which having a characteristic equation of the form $s(\tau s+1)$. Feedback control is needed to stabilize the joint. This is provided by measuring the outputs and feeding them through constant gain amplifiers; the typical servo configuration.

Open Loop Response

Several simulation runs were carried out in order to study the open-loop response of the joint. Unit step inputs of motor torques were used throughout. As expected, when the motor torques were equal in magnitude and direction, the response was found to be a pure roll motion at the output member without any pitch motion. Similarly, when the motor torques were equal in magnitude but opposite in direction, the output member underwent a pure pitch motion, without any roll motion. For other combinations of torque inputs, both roll and pitch motions were simultaneously present. These observations confirm the behavior that is expected from the actual joint.

For example, consider the response of the joint when subjected to unit-step motor torques that are applied in the same direction. The torque response T_1 at one drive roller is shown in Figure 5. The torque response T_2 at the other drive roller is shown in Figure 6. The roll response of the output member is shown in Figure 7. In this case the pitch response will be practically zero. If, however, the motor torques are applied in opposite directions, the roll response will be zero and the pitch response will be similar to what is shown in Figure 7. Note that the slope of the angular response curve becomes constant eventually. This is the steady-state condition of constant speed. Under this condition, the torques at various locations of the joint are utilized exclusively to overcome damping. Damping torques are distributed in such a manner that large torques appear at high-speed components of the traction drive and small torques at low-speed components. Accordingly, with the speed ratios used in the present simulation, most of the damping torque will be concentrated near the two motors. Initially a large torque is needed to accelerate the low-speed components such as the output side of the drive rollers, but eventually these torques will settle down to small values. This explains the shapes of the torque response curves given in Figure 5 and Figure 6.

If the speed reductions are eliminated, the torque distribution will become more uniform. For example, results obtained using $n_R = 1$ and $n_1 = 1$, and for a motor torque of 1.0 oz.in, indicated that in this case the torque at the drive roller output reaches a peak of about 1.2 oz.in and eventually settles down to a value of about 0.5 oz.in. Naturally, the speed distribution will also depend on the values of n_R and n_1.

Several more simulations were carried out to study the effects of other types of parameters on the joint response. Notably, when damping is increased the steady-state roll and pitch speeds reduce in proportion. In particular, if all

damping constants are increased by a factor of 10 while keeping the other parameters the same, the eigenvalues of the open-loop system become:

$$
\begin{array}{l}
-0.25 \pm j\ 677.10 \\
-0.25 \pm j\ 659.48 \\
-0.75 \\
-0.75 \\
\ \ 0.0 \\
\ \ 0.0
\end{array}
$$

Note that the stable eigenvalues have become more stable while the zero eigenvalues are not affected. In particular, the real parts of the eigenvalues have increased by approximately a factor of 10 while the natural frequencies are virtually unchanged. The torque distribution will also be affected by this, large increases being noted at high-speed components.

When the stiffness of the drive rollers is decreased, the primary frequency of the torque response decreases, while the roll and pitch motion responses remain almost unaffected. For example if the stiffness is decreased by a factor of 10 (i.e., K = 3000 oz.in/rad), keeping the other parameter values unchanged, the open-loop eigenvalues of the joint become:

$$
\begin{array}{l}
-0.03 \pm j\ 214.12 \\
-0.02 \pm j\ 208.55 \\
-0.07 \\
-0.07 \\
\ \ 0.0 \\
\ \ 0.0
\end{array}
$$

Here the natural frequencies of the complex eigenvalues have been reduced by a factor of approximately $\sqrt{10}$ while the real eigenvalues are not influenced. It follows that the natural frequencies of the joint are directly affected by the stiffness of the drive rollers.

CONTROL CONSIDERATIONS

Servo Control

In the study outlined above it was noted that the traction-drive joint was completely controllable. Furthermore, it was noted that the joint was completely observable with just the roll angle and the pitch angle as outputs. It follows that the joint can be servo controlled using roll and pitch feedbacks alone. But since torques transmitted through the drive rollers are also measured, all four output variables can be used in the feedback controller design for the joint.

To illustrate the level of improvement that is realizable under servo control, a linear quadratic regulator (LQR) is designed for the joint using complete state feedback. A similar performance level is possible with feedback of the roll and pitch angles alone because the states are completely observable even with these two outputs.

The performance index that is minimized in the design is

$$\text{P.I.} = \int_0^\infty [\underline{x}^T \underline{R}_x \underline{x} + \underline{u}^T \underline{R}_u \underline{u}]dt \qquad (45)$$

with

$$\underline{R}_x = \text{diag}\ (0.,\ 0.,\ 0.,\ 0.,\ 1.0,\ 0.,\ 1.0,\ 0.)$$

$$\underline{R}_u = \text{diag}\ (0.05,\ 0.05)$$

This provides a constant-gain feedback controller of the form:

$$\underline{u} = \underline{K}\ \underline{x} \tag{46}$$

The optimal gain matrix is given by

$$\underline{K} = \begin{bmatrix} 0.0281 & 0.0445 & 0.0 & 0.0 & 0.0055 & 0.0091 & 0.0057 & 0.0095 \\ 0.0 & 0.0 & 0.0281 & 0.0445 & 0.0055 & 0.0091 & -0.0057 & -0.0095 \end{bmatrix}$$

When this controller is included in the joint, the step response of the roll angle becomes as shown in Figure 8. This should be compared with the open-loop step response shown in Figure 7, which was obtained under the same (step) torque input. In particular, good rise time has been achieved without introducing a large overshoot. Also, fast settling to the steady-state angle is seen. The eigenvalues of the closed-loop joint are computed to be:

$$-0.03 \pm j\ 677.10$$
$$-0.02 \pm j\ 659.48$$
$$-0.59 \pm j\ \ 0.59$$
$$-0.59 \pm j\ \ 0.59$$

Note that the free integrators in the open-loop joint have been modified to a stable pair of complex eigenvalues. The stable pair of real eigenvalues in the open-loop joint has also been transformed into a stable complex pair. It can be concluded that satisfactory performance of the traction-drive joint would be possible with a suitable joint servo using at least roll and pitch angle feedback.

Dynamic Coupling and Nonlinearities

The foregoing study reveals that a traction-drive unit can provide a reasonably well-behaved manipulator joint. Independently operating, each joint will behave in a desired manner under servo control. When several such joints are used in a single robot, there will be unavoidable dynamic coupling among joints. Due to these interactions, accurate performance of the manipulator will not be possible in general if the joints are controlled independently. Dynamic performance of the manipulator can be improved by employing a control scheme that takes into account dynamic interactions among joints. Another factor that would need attention is the nonlinear nature of the manipulator. There are three basic sources of nonlinearity in a manipulator; dynamic nonlinearities, geometric nonlinearities, and physical nonlinearities. Dynamic nonlinearities arise due to nonlinear acceleration terms such as coriolis and centrifugal accelerations that are unavoidable in general. Geometric nonlinearities will be present due to the nonlinear geometric transformations that would be necessary in formulating the kinematics of a multi-degree-of-freedom manipulator. To explain this source of nonlinearity, note that what is usually specified is the end effector motion of a robotic manipulator. The corresponding joint motions have to be determined. The motion of a particular link relative to the adjoining link can be expressed as a transformation matrix that

contains trigonometric functions of the corresponding joint variable. These nonlinear terms (trigonometric functions) appear in the overall relationship between the end effector motion and the joint motions. Physical nonlinearities manifest themselves in such forms as coulomb friction and backlash. Effects of nonlinearities are neglected when linear control techniques are used in the analysis and design of joint servos, and this can produce serious errors. Furthermore, for accurate performance, unknown dynamic effects including link flexibility and unmodeled motor characteristics should be compensated through control. Also important is the uncertainty of parameter values. Measurement errors, signal noise, and external disturbances are factors that can degrade the performance of any control system.

Multivariable control techniques that are conventionally classified as "modern control" are very effective in compensating for dynamic interactions, nonlinearities, unknown dynamics, parameter errors, signal noise, and external disturbances. Many multivariable control methods have been proposed for robotic manipulators. These include adaptive control, nonlinear feedback control, variable structure control, and heuristic control strategies. In model-referenced adaptive control, the manipulator is forced to follow the response of a reference model subject to the same input, by continuously adjusting the parameters of the feedback controller [6]. In least-squares adaptive control, the parameters of the feedback controller are continuously adjusted employing an accurate model for the manipulator, so that a quadratic error function of the manipulator trajectory is minimized [7]. In nonlinear feedback control, a nonlinear feedback law is used to produce a linear behavior in the manipulator so that linear control loops could be used effectively [8]. In variable structure control or sliding mode control, the state space is partitioned into several subspaces, each having its own control law [9]. Then a controller is switched on depending on the response location of the manipulator in the state space so as to force the response along a desired hypersurface (sliding surface). In heuristic control, control rules developed using some knowledge base, including past experience, expert opinion, and observed performance, are used to control the manipulator when the conditions are vague or not well defined [(fuzzy) or defined in a linguistic manner and when satisfactory hard algorithms cannot be determined for control]. Here control decisions are made by an inference engine depending on the present status of the response (context) by searching the rule base.

Many of these control methods are model-based techniques. The control effort in a model-based technique can be reduced by improving the accuracy of the model. Of course, there are methods such as model-referenced adaptive control that do not depend on a model for the manipulator. Nevertheless, the independent performance of a joint can be used as the reference for the performance of that joint when responding as a component of an overall system (complete manipulator). Even from this point of view, the present study of a single manipulator joint would be useful.

It is known that the type of robots that is considered in the present study will possess redundant kinematics. Ways to utilize kinematic redundancy in an effective and optimal manner should be addressed. One proposition [10] is for the design of end effector trajectories that will minimize the dynamic reactions (interaction) of the manipulator on the supporting structure, say, a space station. Also flexibility (or, dexterity) of manipulation could be improved using kinematic redundancy, for example, in the context of avoiding obstacles and singular configurations of manipulator.

CONCLUSION

This paper presented an evaluation of dynamic characteristics of a prototype traction-drive joint developed by NASA. A dynamic model was developed using the Lagrange formulation. Controllability, observability, stability, and response characteristics of the joint were studied. The joint was found to be controllable using the motor torques as inputs. The joint was found to be observable with the roll (yaw) and pitch outputs alone. Hence, the measurement of the entire state vector is not necessary for achieving the optimal performance. In particular, the torque measurements available in the present joint design, are not needed in theory. Accuracy of the measured torques will play a significant role in determining the utility of these torques in the manipulator control. For example, high noise levels in the torque signals could lead to instabilities in the manipulator. This is particularly true because torque signals are high-bandwidth measurements that should occupy inner feedback loops whereas the motion signals are relatively low-bandwidth measurements. These torque measurements have practical benefits, however, particularly in hybrid force-motion control. This method of control is known to be effective in manipulations under motion constraints and in fine manipulation. Furthermore, control bandwidth can be improved by employing torque sensing in the control system. But torque measurements alone cannot provide a satisfactory control system, in practice. The joint was found to be marginally stable without servo control, as anticipated. A linear quadratic regulator (LQR) was implemented on the joint to determine a basis for evaluating the performance of the joint under servo control. The response of the joint was found to be quite satisfactory under LQR control. In particular good stability characteristics were observed. Rise time, overshoot, and settling time were also found to be acceptable.

In evaluating the performance of a manipulator that employs more than one traction drive joint in a coordinated manner, several factors that have not been included in our final analysis have to be considered. In particular, various types of nonlinearities (e.g., coriolis and centrifugal accelerations, kinematic nonlinearities, and coulomb friction), dynamic coupling among joints, external disturbances, and parameter errors can have a significant influence on the performance of the robot.

ACKNOWLEDGMENTS

The work reported in this paper was carried out under a NASA-ASEE Fellowship awarded to Dr. C. W. deSilva, during the summer of 1987.

REFERENCES

1. deSilva, C. W.: "Control Sensors and Actuators," Prentice-Hall, Inc., Englewood Cliffs, New Jersey, 1988 (in press).

2. Asada, H., and Youcef-Toumi, K.: "Analysis and Design of a Direct-Drive Arm with a Five-Bar-Link Parallel Drive Mechanism," Proceedings of the 1984 American Control Conference, San Diego, California, pp. 1224-1230, June 1984.

3. Kanade, T. and Schmitz, D.: "Development of CMU Direct-Drive Arm II," Report No. CMU-RI-TR-85-5, Robotics Institute of Carnegie Mellon University, Pittsburgh, Pennsylvania, March 1985.

4. Martin, H. L., Kuban, D. P., Herndon, J. N., Williams, D. M., and Hamel, W. R.: Recommendations for the Next-Generation Space Telerobot System, Report No. ORNL/TM-9951, Oak Ridge National Labortory, Oak Ridge, Tennessee, March 1986.

5. Friedland, B.: Control Systems Design, McGraw-Hill Book Company, New York, 1986.

6. Dubowski, S. and DesForges, D. T.: "The Application of Model-Referenced Adaptive Control to Robotic Manipulators," Journal of Dynamic Systems, Measurement, and Control, Trans. ASME, Vol. 101, pp. 193-200, September 1979.

7. deSilva, C. W. and VanWinssen, J.: "Least Squares Adaptive Control for Trajectory Following Robots," Journal of Dynamic Systems, Measurement, and Control, Trans. ASME, Vol. 109, No. 2, pp. 104-110, June 1987.

8. Tourassis, V. D. and Neuman, C. P.: "Robust Nonlinear Feedback Control for Robotic Manipultors," IEEE Proceedings, Vol. 132, No. 4, pp. 134-143, July 1985.

9. Slotline, J. J. E.: "The Robust Control of Robot Manipultors," The International Journal of Robotics Research, Vol. 4, No. 2, pp. 49-64, Summer 1985.

10. deSilva, C. W., Chung, C. L., and Lawrence, C.: "Base Reaction Optimization of Manipulators for Space Applications," Proceedings of the International Symposium on Robots, Sydney, Australia, November 1988.

e Arm

17647 N89-14006 (NASA-TM-101499) DYNAMIC EVALUATION OF A TRACTION-DRIVE JOINT FOR SPACE TELEROBOTS Clarence W. deSilva (British Columbia Univ., Vancouver.) et al.(NASA) Oct. 1988 31 p G3 G 63
NAS 1.15:101499
Unclas

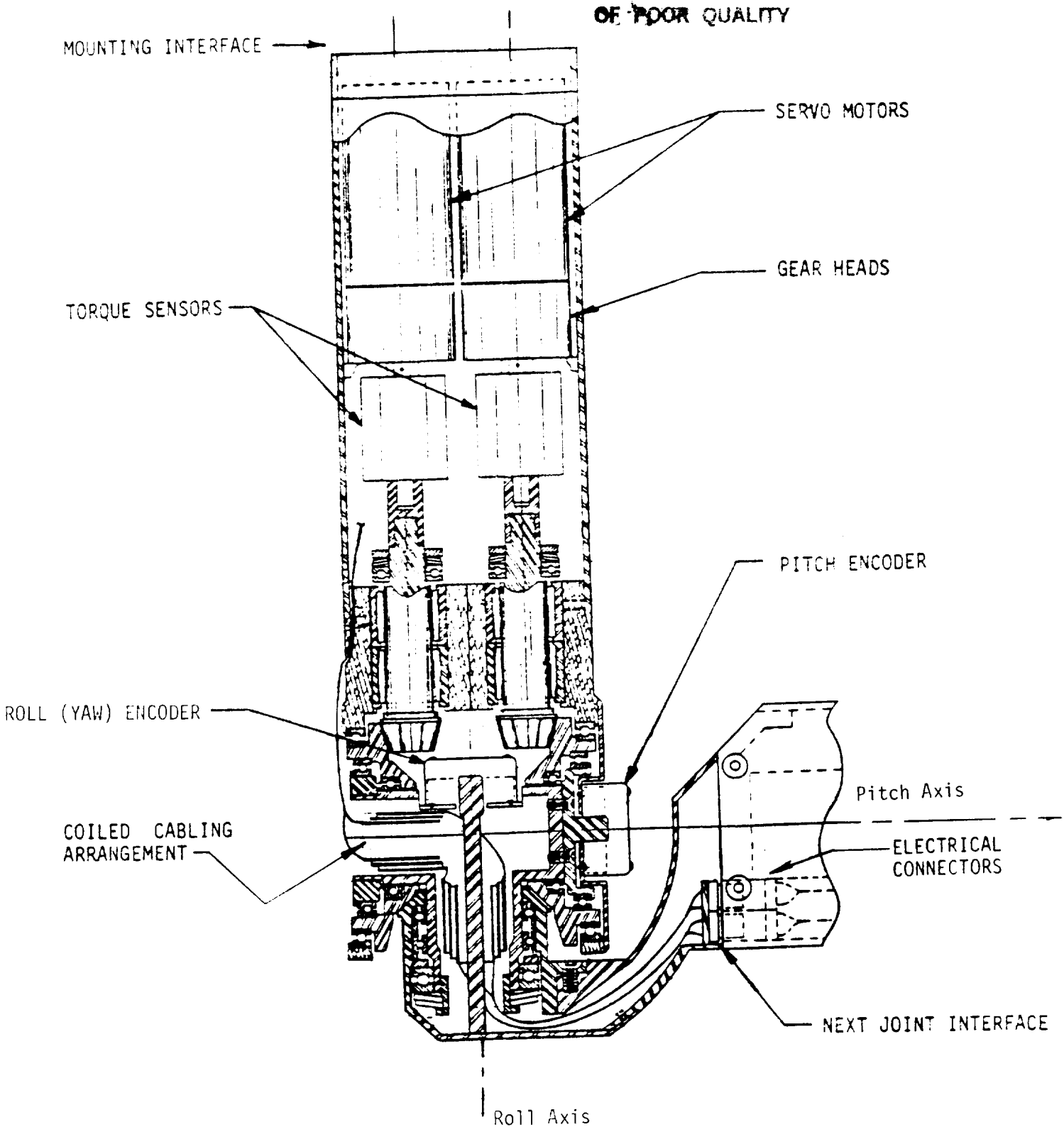

Figure 2.- Details of a Typical Traction-Drive Joint

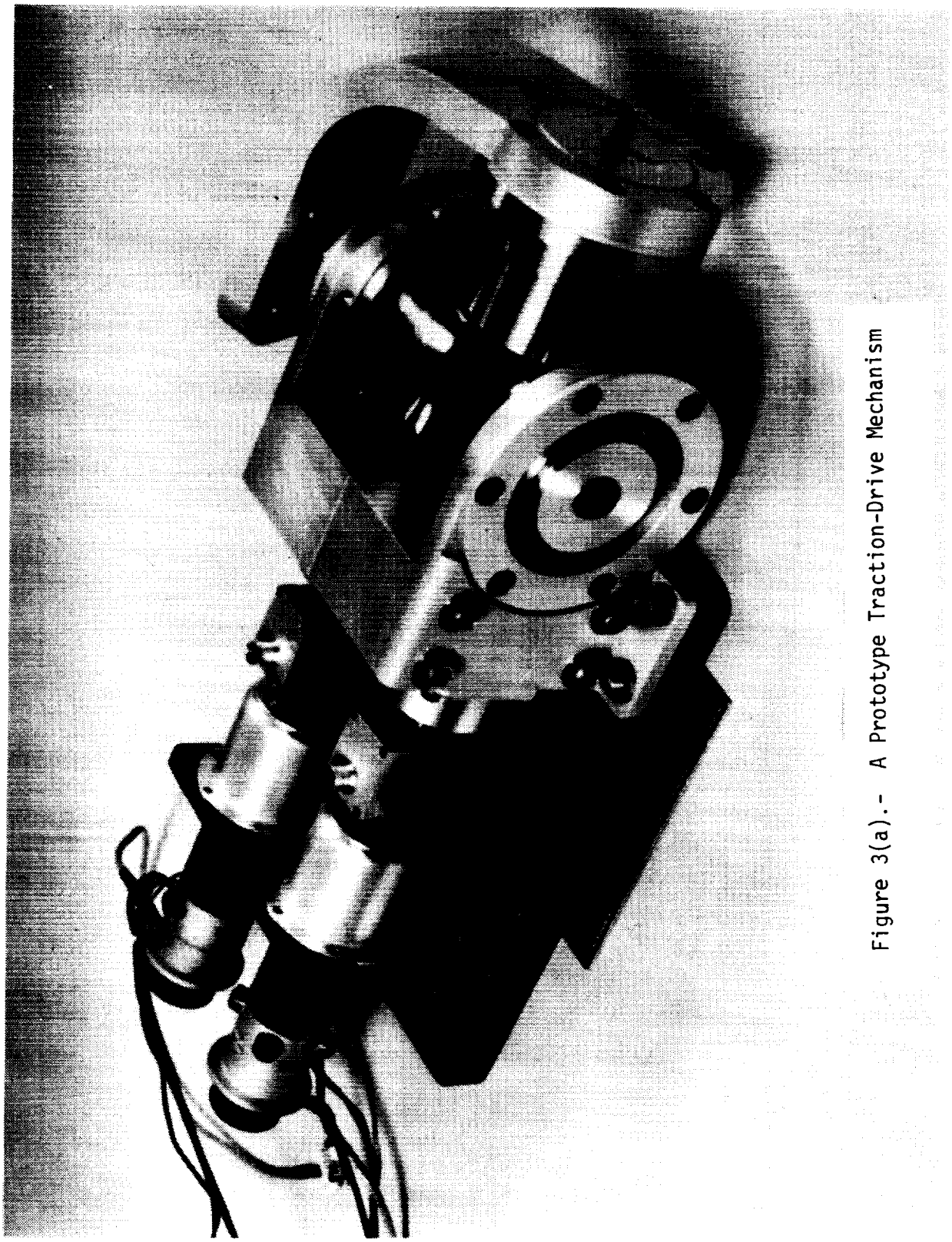

Figure 3(a).- A Prototype Traction-Drive Mechanism

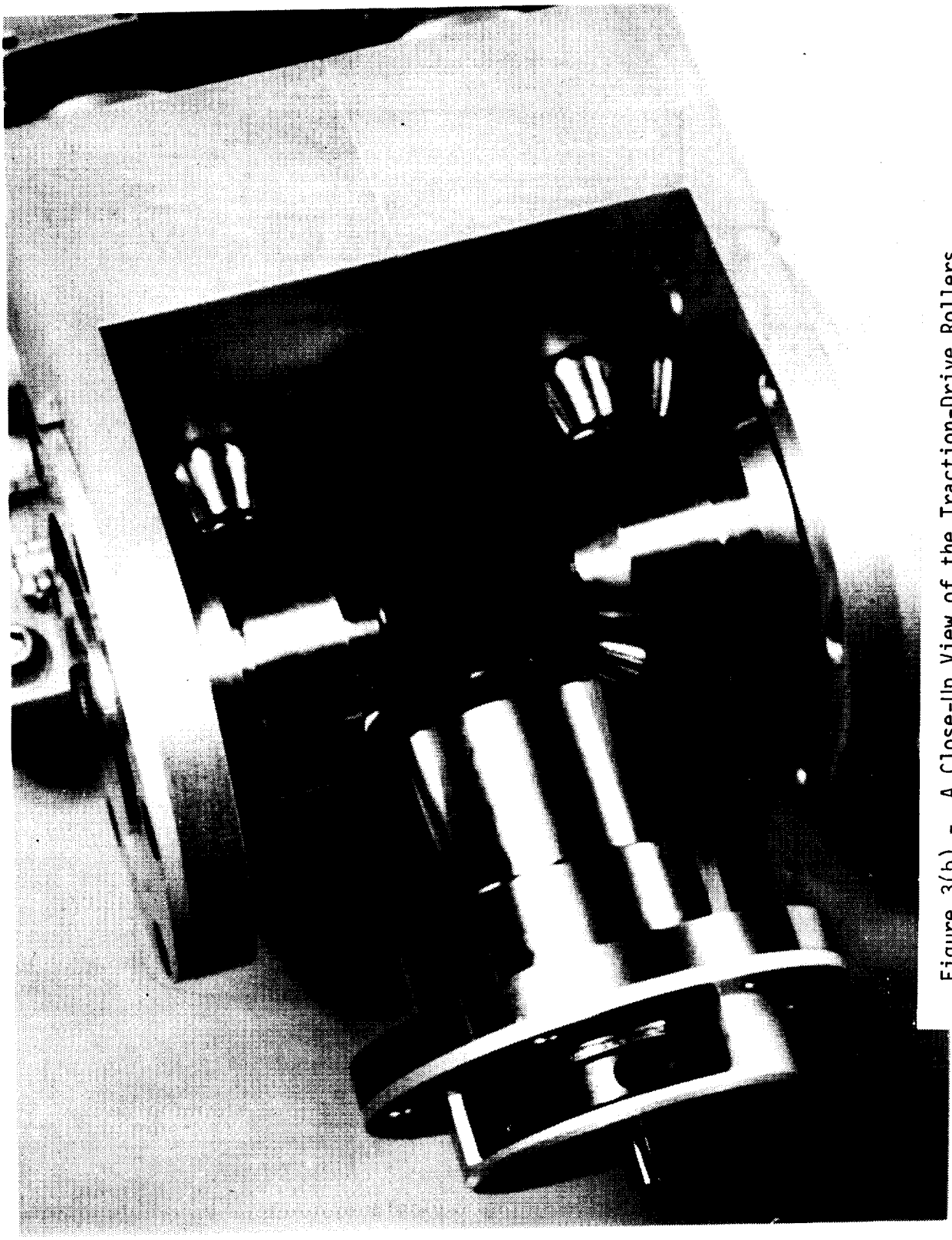

Figure 3(b).- A Close-Up View of the Traction-Drive Rollers

J = Moment of inertia
b = damping constant
K = stiffness
T = torque
n = gear ratio

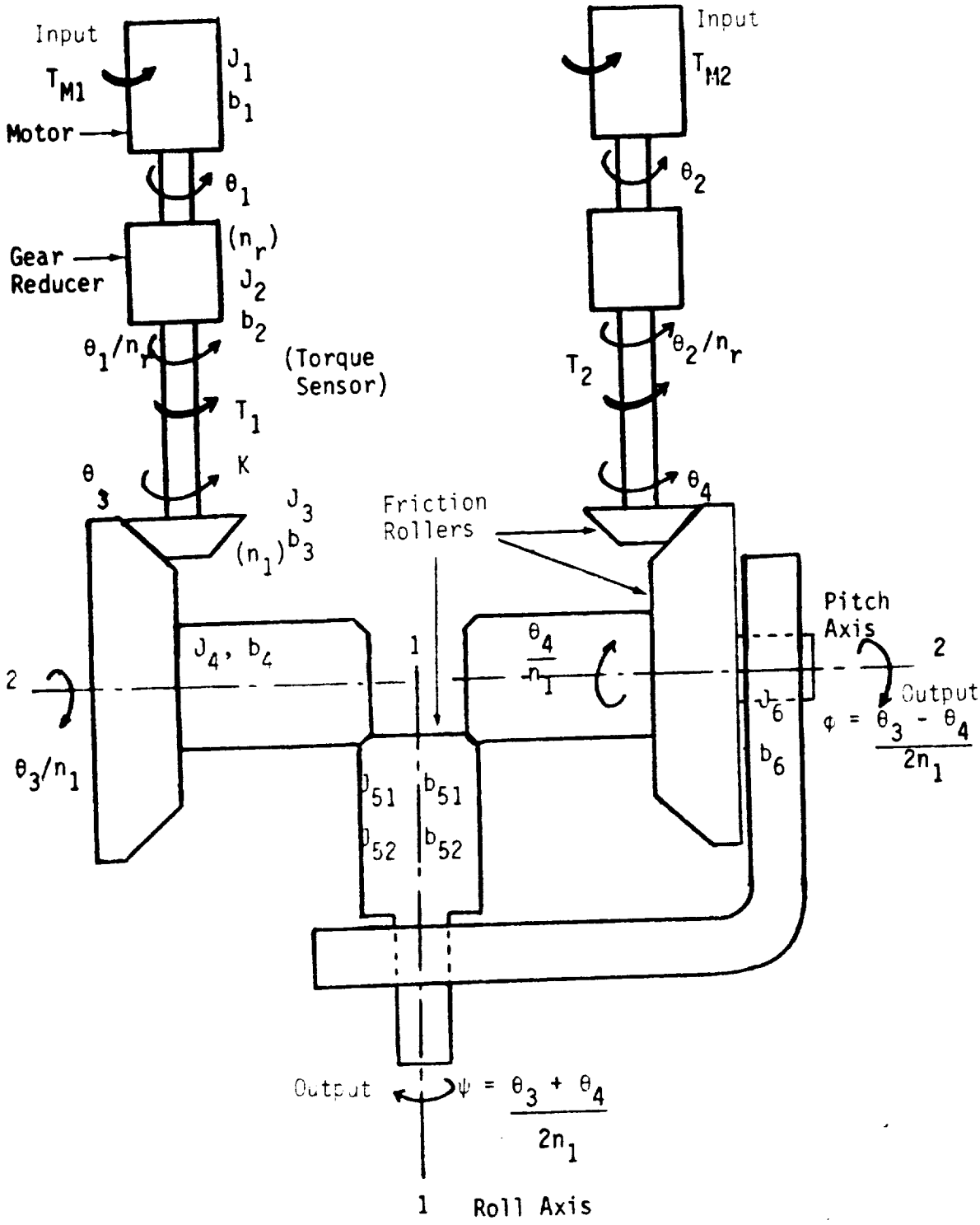

Figure 4.- A Dynamic Model for the Traction-Drive Joint

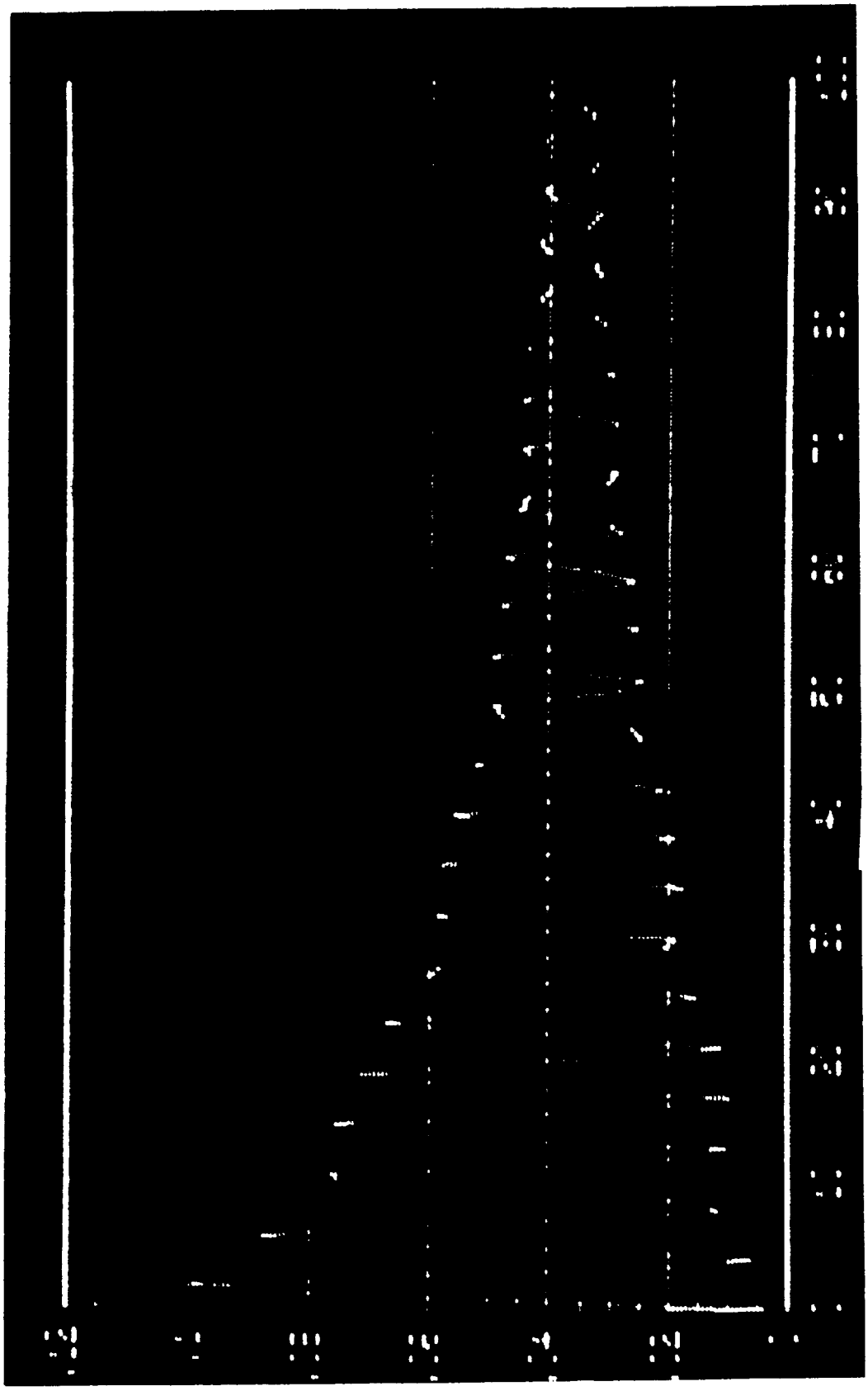

Figure 5.- Step Response of the Torque Through a Drive Roller

Figure 6.- Step Response of the Torque Through the Second Roller

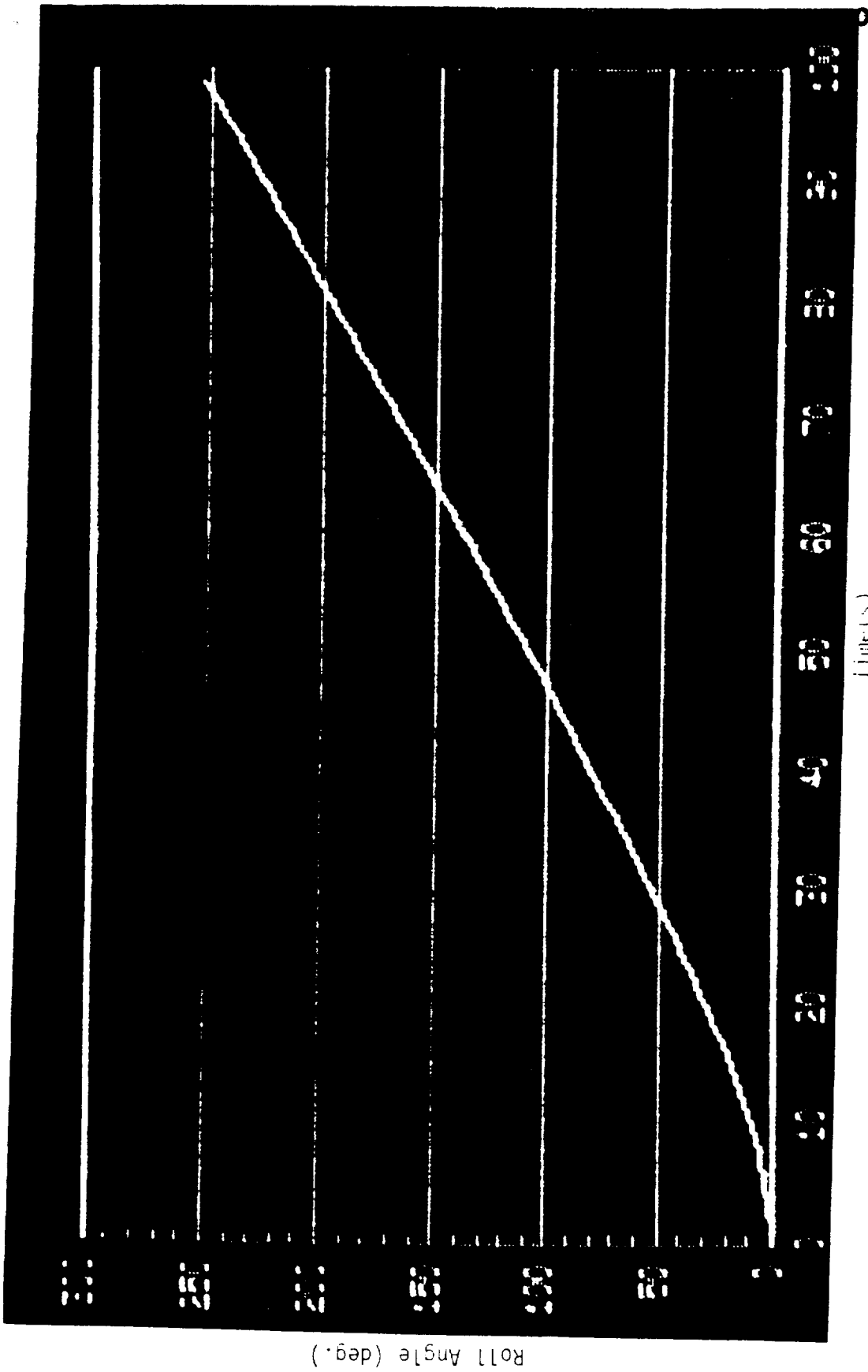

Figure 7.- Step Response of the Roll Angle of the Output Member

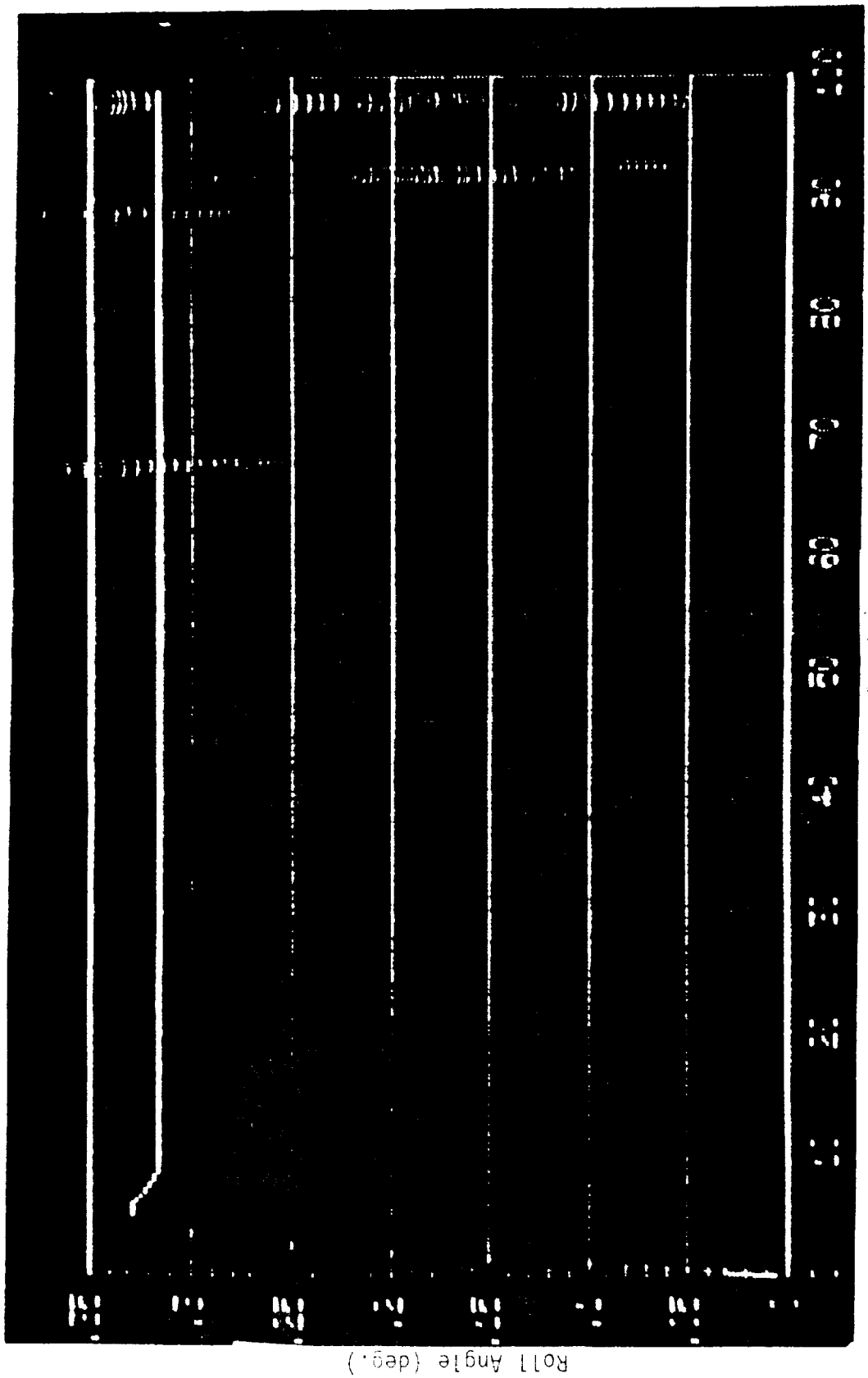

Figure 8.- Step Response of the Roll Angle Under Feedback Control

Report Documentation Page

1. Report No.	2. Government Accession No.	3. Recipient's Catalog No.
NASA TM-101499		

4. Title and Subtitle	5. Report Date
Dynamic Evaluation of a Traction-Drive Joint for Space Telerobots	October 1988
	6. Performing Organization Code

7. Author(s)	8. Performing Organization Report No.
Clarence W. deSilva* and Walter W. Hankins III	
	10. Work Unit No. 549-02-41-01

9. Performing Organization Name and Address	11. Contract or Grant No.
NASA Langley Research Center Hampton, VA 23665-5225	
	13. Type of Report and Period Covered: Technical Memorandum

12. Sponsoring Agency Name and Address	14. Sponsoring Agency Code
National Aeronautics and Space Administration Washington, DC 20546-0001	

15. Supplementary Notes

*NSERC Professor of Industrial Automation, Department of Mechanical Engineering, University of British Columbia

16. Abstract

This paper presents an analysis and evaluation of a prototype traction-drive joint for robotic manipulators, developed under the sponsorship of NASA. A dynamic model is developed using the Lagrange formulation. Controllability, observability, dynamic stability, and response characteristics of the joint to test inputs are studied. A linear quadratic regulator (LQR) is implemented on the joint model to determine a basis for evaluating the performance of the traction-drive joint under servo control. An evaluation of the results and directions for future investigations are presented.

17. Key Words (Suggested by Author(s))	18. Distribution Statement
Traction-drive joint Manipulator control Linear quadratic regulator Servo control of robotic joints	Unclassified - Unlimited Subject Category 63

19. Security Classif. (of this report)	20. Security Classif. (of this page)	21. No. of pages	22. Price
Unclassified	Unclassified	30	A03